AA Technical Memorandum NOS 16

DEEP SEA TIDE AND CURRENT OBSERVATIONS IN THE GULF OF ALASKA AND NORTHEAST PACIFIC

Carl A. Pearson

Rockville, Md.
December 1975

noaa NATIONAL OCEANIC AND ATMOSPHERIC ADMINISTRATION / National Ocean Survey

NOAA TECHNICAL MEMORANDA

National Ocean Survey Series

(NOS) provides charts and related information for the safe navigation of The survey also furnishes other Earth science data--from geodetic, hydro-magnetic, seismologic, gravimetric, and astronomic surveys or observations, ements--to protect life and property and to meet the needs of engineering, ustrial, and defense interests.

NOAA Technical Memoranda NOS series facilitate rapid distribution of material that may be preliminary in nature and which may be published formally elsewhere at a later date. Publications 1 through 8 are in the former series, ESSA Technical Memoranda, Coast and Geodetic Survey Technical Memoranda (C&GSTM). Beginning with 9, publications are now part of the series, NOAA Technical Memoranda NOS.

Publications listed below are available from the National Technical Information Service (NTIS), U.S. Department of Commerce, Sills Bldg., 5285 Port Royal Road, Springfield, Va. 22151. Price varies for paper copy; $2.25 microfiche. Order by accession number (in parentheses) when given.

ESSA Technical Memoranda

C&GSTM 1 Preliminary Measurements With a Laser Geodimeter. S. E. Smathers, G. B. Lesley, R. Tomlinson, and H. W. Boyne, November 1966. (PB-174-649)

C&GSTM 2 Table of Meters to Fathoms for Selected Intervals. D. E. Westbrook, November 1966. (PB-174-655)

C&GSTM 3 Electronic Positioning Systems for Surveyors. Angelo A. Ferrara, May 1967. (PB-175-604)

C&GSTM 4 Specifications for Horizontal Control Marks. L. S. Baker, April 1968. (PB-179-343)

C&GSTM 5 Measurement of Ocean Currents by Photogrammetric Methods. Everett H. Ramey, May 1968. (PB-179-083)

C&GSTM 6 Preliminary Results of a Geophysical Study of Portions of the Juan de Fuca Ridge and Blanco Fracture Zone. William G. Melson, December 1969. (PB-189-226)

C&GSTM 7 Error Study for Determination of Center of Mass of the Earth From Pageos Observations. K. R. Koch and H. H. Schmid, January 1970. (PB-190-982)

C&GSTM 8 Performance Tests of Richardson-Type Current Meters: I. Tests 1 Through 7. R. L. Swanson and R. H. Kerley, January 1970. (PB-190-983)

NOAA Technical Memoranda

NOS 9 The Earth's Gravity Field Represented by a Simple Layer Potential From Doppler Tracking of Satellites. Karl-Rudolf Koch and Bertold U. Witte, April 1971. (COM-71-00668)

NOS 10 Evaluation of the Space Optic Monocomparator. Lawrence W. Fritz, June 1971. (COM-71-00768)

NOS 11 Errors of Quadrature Connected With the Simple Layer Model of the Geopotential. Karl-Rudolf Koch, December 1971. (COM-72-10135)

NOS 12 Trends and Variability of Yearly Mean Sea Level 1893-1971. Steacy D. Hicks, March 1973. (COM-73-10670)

NOS 13 Trends and Variability of Yearly Mean Sea Level 1893-1972. Steacy D. Hicks and James E. Crosby, March 1974. (COM-74-11012)

NOS 14 Some Features of the Dynamic Structure of a Deep Estuary. Michael Devine, April 1974. (COM-74-10885)

NOS 15 An Average, Long-Period, Sea-Level Series for the United States. Steacy D. Hicks and James E. Crosby, September 1975. (COM-75-11463)

NOAA Technical Memorandum NOS 16

DEEP SEA TIDE AND CURRENT OBSERVATIONS IN THE GULF OF ALASKA AND NORTHEAST PACIFIC

Carl A. Pearson

Rockville, Md.
December 1975

UNITED STATES
DEPARTMENT OF COMMERCE
Rogers C. B. Morton, Secretary

NATIONAL OCEANIC AND
ATMOSPHERIC ADMINISTRATION
Robert M. White, Administrator

National Ocean
Survey
Allen L. Powell, Director

Mention of a commercial company or product does not constitute an endorsement by the NOAA National Ocean Survey. Use for publicity or advertising purposes of information from this publication concerning proprietary products or the tests of such products is not authorized.

CONTENTS

DEEP SEA TIDE AND CURRENT OBSERVATIONS IN THE GULF OF ALASKA AND NORTHEAST PACIFIC

Carl A. Pearson
Oceanographic Division, National Ocean Survey, NOAA
Rockville, Maryland

ABSTRACT. Tide and current records from three deep sea stations in the Gulf of Alaska and northeast Pacific are examined. Deep sea tidal amplitudes are approximately equal to those of adjacent shore locations. The tide wave appears to be a progressive wave traveling northward parallel to the continental slope.

INTRODUCTION

Until recently, knowledge of tides of the ocean has been based almost solely on observations taken along the coast. Unfortunately, coastal tides are greatly influenced by local topography and prevalent weather conditions. Measurement of deep sea tides is essential to the understanding of the dynamics of continental shelf circulation, but logistic and technological problems have prevented any extensive observational programs.

In 1972 the National Ocean Survey (NOS) began a limited program for the measurement of offshore tides and initially deployed two deep sea tide and current measuring systems in the Gulf of Alaska from the NOAA Ship SURVEYOR. The gages were located to the south of Middleton Island, in line with the entrance to Prince William Sound. An objective of the project was to help define the tide wave in its transition from the deep sea across the continental shelf. This is considered an important area as Prince William Sound is to become the terminus for a trans-Alaska pipeline, and a knowledge of the tides of the region will be imperative with the expected large increase in tanker traffic.

Another system was deployed by the NOAA Ship OCEANOGRAPHER while conducting various oceanographic investigations off the coast of Vancouver Island in 1973. This area is near the approaches to the Strait of Juan de Fuca, another area of increasing tanker traffic.

The tide and current information obtained in both areas, especially in the Gulf of Alaska, has become increasingly relevant in light of the research now being conducted over the

continental shelves in relation to future development of oil reserves.

Deployment sites of the deep sea tide and current measuring system are shown in figure 1. Table 1 shows the position, depth, dates of installation and retrieval, and lengths of the tide and current series.

INSTRUMENTATION

The tide gages used during this project are equipped with a Bourdon tube pressure transducer with a frictionless optical readout (described by Filloux 1970, 1971). Relative pressure was recorded 10 times per hour on a strip-chart recorder controlled by an Accutron timer. Richardson-type film recording current meters were also used; the sampling rate was 6 times per hour in the 1972 installations and 4 times per hour in 1973.

Figure 2 shows the mooring configuration used. The tide gage is housed in a 66-cm internal diameter aluminum sphere mounted on an aluminum instrument base. Flanking the tide gage are two AMF acoustic release transponders. A steel bar bridges the release mechanisms of the transponders, and is connected by a chain to the anchor base tripod in such a way that if either release fires, the instrument base is freed from the tripod. Floatation is provided by a syntactic foam buoy connected to the instrument base by 37 m of cable. The current meter is suspended directly beneath the buoy.

DATA REDUCTION

The Accutron timers in the tide gages showed a tendency to drift at a rate of about 2 to 4 minutes per month. Time drift was determined by checking the time just before deployment and upon recovery, and was corrected by assuming a linear drift rate. Laboratory tests have since confirmed the linear drift rate. Data were tabulated at 1-hour intervals for the Gulf of Alaska stations. The interval was 1/2-hourly for the Vancouver Island station due to the short duration of record.

The Bourdon tube is subject to creep resulting from the intense abyssal pressures at operating depth. The creep, which has been found empirically to approximate a logrithmic curve, results in an apparent gradual monotonic increase in sea level pressure. The rate of creep, usually about 50 to 100 mb during the first month of deployment, decreases with time. The creep was removed by fitting the data by least squares to the curve

$$Y = A + B \ln (\Delta T) ,$$

where Y is the creep curve in mb, and ΔT is the time elapsed in hours since the gage was emplaced on the ocean bottom. This curve was then subtracted from the data, after which a preliminary analysis was performed and the residual series was scanned to detect tabulation errors.

The current meter timers had a greater drift rate which was also assumed to be linear. Data were low passed with a cutoff period of approximately three hours to prevent aliasing in the analysis, and decimated to one point per hour.

QUALITY OF DATA RECOVERED

The lengths of the series obtained are shown in table 1. The deep Gulf of Alaska deployment (station 1) and that off Vancouver Island (station 3) both provided tide data of excellent quality. The gage on the shelf near Middleton Island (station 2) was subject to wave noise of a few centimeters amplitude. In addition, there seems to have been a malfunction in the sensing or recording mechanism of the gage, so the reliability of the data is open to question. Since stations 1 and 2 were quite close together, and a preliminary analysis indicated little difference in the tidal constants, the analysis of tides at station 2 has been omitted from this report.

The current meter at station 2 operated satisfactorily for almost 34 days before running out of film. At station 1, the current meter stopped measuring speed after about 2 days, possibly because of the cold temperatures and low current speeds. However, it continued to record current direction. At station 3, the current meter operated properly during all 18 days of deployment.

GENERAL DESCRIPTION OF TIDES AND CURRENTS IN THE REGION

Tides in the northeast Pacific and Gulf of Alaska are mixed, predominantly semidiurnal, with the ratio;

$$\frac{K_1 + O_1}{M_2 + S_2} \cong 0.5.$$

This area is part of the northeast Pacific semidiurnal amphidromic system, although the various empirical and mathematical tidal models differ greatly in the location of the amphidrome (Hendershott 1973). The tide crest propogates in a counterclockwise direction, or northerly along the North American

coast. The mean daily tidal range increases from about 1.7 m at Cape Mendocino, to 2.4 m at Cape Flattery, to over 3.0 m at Sitka and the northern Gulf of Alaska.

The Aleutian Subarctic (or North Pacific) Current sets to the east and divides into two branches at approximately 48°N before reaching the North American Continent (fig. 1). One branch sets to the south as the California Current and the other to the north to become part of the counterclockwise gyre in the Gulf of Alaska known as the Alaska Current (Sverdrup et al. 1942).

Figures 3 and 4 show plots of 15-day sections of the tide and current series. Figure 3 shows the hourly tide at the deep Middleton Island station (station 1), and the filtered hourly currents at the shallow site (station 2). Figure 4 gives the 1/2-hourly tide and filtered hourly current plots at station 3.

The semidiurnal characteristic is evident in both the tides and currents. The negative trend in the plot of the east component of the current at station 2 (fig. 3) is a manifestation of the westerly drift of the Alaskan Current.

TIDAL ANALYSIS

The data were analyzed for tidal components by the response method (Munk and Cartwright 1966), using a procedure of analysis based on that suggested by Cartwright et al. (1969). For the analysis of deep sea tides, the response method gives results slightly better than those obtained by traditional harmonic methods (B. Zetler, personal communication). It also has a certain physical advantage in that it measures the ocean's response to the gravitational potential itself, rather than analyzing the data for a set of predetermined frequencies.

In this study a complex reference series was computed using the second-degree expansion of the gravity potential. For the analysis of short term pelagic series, Cartwright et al. (1969) recommended the use of a complex reference derived from a long series for a nearby coastal station. Tofino (Vancouver I.) was chosen for this purpose. Therefore, the gravitational potential formed a reference for predicting a complex Tofino series, which became the reference in the analysis of the deep sea records. Complex predictions of the deep sea tide records then became the references for the respective current stations. Note that the deep sea tide records are in millibars while the reference series are in centimeters. Therefore, the admittance amplitudes are not true admittances, but rather the admittance times the ratio of mb/cm. The same applies to the current admittances which include the ratio

$$\text{cm s}^{-1}\ \text{mb}^{-1}.$$

TIDES

Tables 2 to 6 show the results of the analyses, giving the response admittances (ratio of station tide to reference input) and harmonic constants derived from the admittances. Table 2 gives the constituents of the Tofino reference tide. Table 3 shows the results of the analysis for the nearby tide station 3. Semidiurnal admittance amplitudes are close to unity, while there is some amplification in the diurnal band. Phases at the deep sea location tend to lead Tofino for both species, probably because of delay across the continental shelf.

The analysis for deep sea tide station 1 in the Gulf of Alaska is given in Table 4. Both species show an amplification over station 3, and both have a phase delay of about 1.5 hours relative to station 3.

The amplitudes at both deep sea stations are comparable to those at nearby shore stations. For example, M_2 at station 1 is 108.8 mb (111 cm), while at Sitka it is 109.5 cm, Yakutat 111.5 cm, and Kodiak only 94.7 cm. K_1 is 48.4 mb (49 cm) at the deep sea station, 45.5 cm at Sitka, 45.2 cm at Yakutat, and 39.0 cm for Kodiak. Thus, there has been no amplification of the semidiurnal tide across the continental shelf, and in fact, the diurnal tide appears to be greater at the deep sea locations than at the shore stations. This probably can be attributed to: the narrow continental shelf, the fact that the tide wave progresses along the coastline rather than running up against it as a standing wave, and the dissipation of energy by the many sounds, inlets, and archipelagoes along the shore of western Canada and around the Gulf of Alaska.

It is of interest to note that the diurnal and semidiurnal gravitational tides account for nearly all the variance (about 99.8 percent) of the deep sea tide records as opposed to 85 percent to 95 percent typical of coastal stations. This is because the deep sea gages are away from the effects of storm surges and other changes in water height which sometimes affect coastal gages. Since the tide gages were in the deep ocean, shallow water constituents are insignificant and wave noise is largely attenuated.

CURRENTS

The progressive vector diagram of station 2 (fig. 5) indicates the predominant southwesterly flow. During the first 3 days the flow was northeasterly; then it reversed and flowed toward the southwest with a mean velocity of 16.5 cm/s at 251^{o}true.

Tables 5 and 6 give the results of the response analysis for the last 29 days of current observations at station 2. No lags were used (because of noise in the current series), resulting in a constant admittance in each species. An estimate of standard error per lunar month, defined by Cartwright et al. (1969) as

$$S.E. = \left(\frac{1}{2} \cdot \frac{\text{residual variance}}{\text{recorded variance}} \cdot \frac{27.3}{\text{days of series}}\right)^{\frac{1}{2}}$$

is given for each species.

The gravitational (diurnal and semidiurnal) tidal currents accounted for about 60 percent of the variance in the north component. In the east component, which had a larger total variance, the gravitational current accounted for 52 percent. The semidiurnal tidal current admittance was about twice that of the diurnal in the north component, while admittances for the east component were approximately equal.

This can be explained by referring to the current ellipses for K_1 and M_2 (fig. 6). The major axis of K_1 has an alinement of 258° true while that of M_2 is 60° true. Therefore the alinement of M_2 is a greater departure from an east-west reference. In addition, the major axis of K_1 is about three times the length of the minor, while for M_2 the ratio is only 2:1. An interesting feature of the current is that both ellipses are alined approximately with the mean current. This is also the approximate alinement of the continental slope in the area (fig. 1), which again indicates that the tide wave progresses along the slope rather than across it.

The phase of the major axis of the M_2 current lags the tide by approximately 1.0 hour, while that of the K_1 leads by 2.5 hours. Admittance amplitudes are approximately equal for both species.

The residual current series was further analyzed for the terdiurnal and quarterdiurnal bilinear interaction constituents. A reference series was formed by multiplying together the terms of the complex predicted diurnal and semidiurnal current series. The terdiurnal series was formed by the product of the diurnal and semidiurnal complex predictions, and the quarterdiurnal series from the square of the complex semidiurnal predictions. For the north component, the bilinear tide accounted for only about 2 $(cm/s)^2$ of the variance. The east component variance was reduced by an additional 17 $(cm/s)^2$ by including the bilinear terms.

A periodogram, showing spectral energy distribution at frequency intervals of 0.03448 cycles per day for the north and

east components of station 2, is given in figure 7. It shows energy at 3 and 4 cycles per day, and at periods of 1 month, 1 week, and about 3 days, in addition to the diurnal and semidiurnal tidal bands. There is no discernable energy at the inertial frequency of 1.7 cycles per day.

DEEP CURRENT STATION

Even though current speed was obtained for only 2 days at the deep station, examination of the data is still worthwhile. Means of the north and east components of the current data over 4 tidal cycles show an average speed of 3.8 cm/s at 009° true. This predominant flow can be seen on the progressive vector diagram of figure 8 which also shows the "cusps" resulting from the tidal signal.

In the relative frequency diagram of figure 8, current speeds are plotted as a function of direction and as the percentage of observations for each 5° of direction. This permits comparison of the direction readings during the 2 days for which speeds were recorded with those over the entire period of observation. The similarity between the relative frequency of direction both for the first 2 days (lines) and for the entire series (circles) is evident. Approximately 50 percent of all observations fall in the northerly quadrant suggesting a near bottom current flowing roughly counter to the Alaskan current at this location.

VANCOUVER ISLAND CURRENTS

The plot for station 3 (fig. 4) indicates a semidiurnal current. However, the strength and phase of the signal vary relative to the tide record. The periodogram of the north and east components of the current is given in figure 9 (frequency interval 0.0667 cycles per day). It indicates a strong broad band semidiurnal peak, centered on M_2 in the north component and S_2 in the east component. The diurnal signal does not appear to rise much above the background noise of either component, nor does there appear to be energy at the inertial frequency of 1.5 cycles per day. A response analysis showed little coherence with the surface gravitational tide. The (apparently) coherent portion of the semidiurnal tidal current accounts for about 45 percent of the variance within the tidal band of the north component, and less than 10 percent of the east component. This is reflected in the M_2 current ellipse (fig. 10) which shows the major axis inclined a little west of north and a very small minor axis. The major axis approximately parallels the continental slope, although the low signal-to-noise ratio introduces a large amount of uncertainty. The computed harmonic constants for M_2 were 2.5 cm/s with a Greenwich phase of 201° for the north component, and 0.9 cm/s, 13° for the east component.

The mean current during the period of observation was about 1 cm/s toward the south-southwest. However, the progressive vector diagram (fig. 11) shows a southwesterly current (downslope) during the first half of the observation, then a shift to south-southeast (parallel to the slope) with the burst of semidiurnal energy beginning on about the ninth day (also see fig. 4).

CONCLUSIONS

The deep sea tide and current data from three locations in the northeast Pacific Ocean and Gulf of Alaska indicate a predominately semidiurnal tide wave which progresses northward parallel to the continental slope. The tidal amplitudes at the two deep sea locations (just seaward of the continental slope) are approximately equal to those at adjacent coastal stations. Tidal current ellipses are alined with the general direction of the continental slope isobaths. In comparing the observed M_2 with global maps published in Hendershott (1973), which was based on a global numerical tidal model, it appears that the Hendershott model best fits the data in the northeast Pacific.

ACKNOWLEDGMENTS

I express my appreciation to the officers and crew of the NOAA Ships SURVEYOR and OCEANOGRAPHER, and personnel of the Engineering Development Laboratory and the Oceanographic Division, NOAA, for their assistance. I am indebted to Mark Wimbush, NOVA University, and Hal Mofjeld, Atlantic Oceanographic and Meteorological Laboratory, NOAA, for their advice and cooperation.

REFERENCES

Cartwright, D., Munk, W., and Zetler, B., "Pelagic Tidal Measurements," Transactions, American Geophysical Union (EOS), Vol. 50, 1969, pp. 472-477.

Filloux, J., "Bourdon Tube Deep Sea Tide Gages," Tsunamis in the Pacific Ocean, W.M. Adams, ed., East-West Center Press, Honolulu, Hawaii, 1970, pp. 223-238.

Filloux, J., "Deep Sea Tide Observations from the Northeastern Pacific," Deep Sea Research, Vol. 18, 1971, pp. 275-284.

Hendershott, M., "Ocean Tides," Transactions, American Geophysical Union (EOS), Vol. 54, No. 2, 1973, pp. 76-86.

Munk, W., and Cartwright, D., "Tidal Spectroscopy and Prediction," Philosophical Transactions of the Royal Society of London, Ser. A., Vol. 259, 1966, pp. 533-581.

Sverdrup H., Johnson, M., and Fleming, R.,"The Oceans," Prentice-Hall, Englewood Cliffs, N.J., 1942.

Table 1.--Positions and lengths of series.

Position no.	Lat.	Long.	Depth (m)	Deployed	Retrieved	Days of tide data	Days of current data
1	58°45.7	145°42.8	4370	7/16/72	8/27/72	41	2*
2	59°22.2	146°13.8	150	7/20/72	8/27/72	34	34
3	48°58.2	127°17.1	1999	8/21/73	9/8/73	18	18

*Directions were recorded for 34 days

Table 2.--Response analysis for Tofino, British Columbia, predicted from 369-day harmonic constants.

Reference: gravitational potential

$C_2^{1,2}$ (0,±48, ±96)

Lat. 49°9N
Long. 125°55W

Frequency (CPD)	Admittance, station to reference REAL	IMAG	Amplitude (R)	Phase lead (°)	Harmonic constituents	Harmonic constants H (cm)	G (°)	K (°)
0.8932	0.4149	-0.6896	0.8048	-59.0				
0.9295	0.4261	-0.8058	0.9116	-62.1	Q_1	4.1	239.0	113.1
0.9661	0.4322	-0.7834	0.8948	-61.1	O_1	23.9	242.1	116.2
0.9973	0.4265	-0.9174	1.0118	-65.1	M_1	1.8	241.1	115.2
1.0027	0.4205	-0.9574	1.0457	-66.3	P_1	12.3	245.1	119.2
1.0393	0.3022	-1.2237	1.2604	-76.1	K_1	38.6	246.3	120.4
	Predicted variance 1194 cm^2				J_1	2.6	256.1	130.2
1.8591	-0.8709	0.7693	1.1620	138.5	μ_2	2.2	221.5	329.7
1.8960	-0.8171	1.4376	1.6535	119.6	N_2	20.0	240.4	348.6
1.9323	-0.2795	1.5356	1.5609	100.3	M_2	98.6	259.7	7.9
1.9689	0.2110	1.2689	1.2863	80.6	L_2	2.3	279.4	27.6
2.0000	0.1656	0.9380	0.9525	80.0	S_2	28.0	280.0	28.2
2.0055	0.1000	0.8775	0.8832	83.5	K_2	7.1	276.5	24.7
	Predicted variance 5437 cm^2							

Total predicted variance 6631.4 cm^2

Table 3.--Response analysis for deep sea tide station 3, in millibars.
(Reference series in centimeters)

Reference: "Predicted" Tofino tide

$X_2^{1,2}$ $(0,\pm 48)$

August 22, 1973 to September 8, 1973
(17.6 days)

Lat. 48°58.2N
Long. 127°17.1W
Depth 1999 meters

Frequency (CPD)	Admittance, station to reference REAL	IMAG	Amplitude (R)	Phase lead (°)	Harmonic constituents	Harmonic constants H (mb)*	G (°)	K (°)
0.8932	1.1646	0.3450	1.2146	16.5				
0.9295	1.1473	0.3142	1.1895	15.3	Q_1	4.9	222.5	95.2
0.9661	1.1423	0.2104	1.1616	10.4	O_1	28.4	226.8	99.5
0.9973	1.1489	0.0805	1.1518	4.0	M_1	2.1	230.7	103.4
1.0027	1.1511	0.0552	1.1524	2.7	P_1	14.2	241.1	113.8
1.0393	1.1716	-0.1192	1.1777	-5.8	K_1	44.4	243.6	116.3
	Predicted variance 1325 mb^2		SE = 1.4%	0.8°	J_1	3.1	261.9	134.6
1.8591	0.8819	0.5342	1.0311	31.2				
1.8960	0.8982	0.4484	1.0039	26.5	μ_2	2.3	190.3	295.7
1.9323	0.9271	0.3521	0.9917	20.8	N_2	20.1	213.9	319.3
1.9689	0.9632	0.2630	0.9984	15.3	M_2	97.8	238.9	344.3
2.0000	0.9937	0.2075	1.0151	11.8	L_2	2.3	264.1	9.5
2.0055	0.9987	0.2005	1.0186	11.4	S_2	28.4	268.2	13.6
	Predicted variance 5349 mb^2		SE = 0.9%	0.5°	K_2	7.2	265.1	10.5

*1.00 mb ≈ 1.01 cm sea water

Total recorded variance	6688.04 mb^2
Total predicted variance	6674.22 mb^2 = 99.79%
Residual variance	13.82 mb^2

Table 4.--Response analysis for deep sea tide station 1 (south of Middleton I.), millibars.
(Reference series in centimeters)

Reference: "Predicted" Tofino tide

July 18, 1972 to August 26, 1972
(40 days)

$X_2^{1,2}$ (0, ±48)

Lat. 58°45.7N
Long. 145°42.8W
Depth 4370 meters

Frequency (CPD)	Admittance, station to reference REAL	IMAG	Amplitude (R)	Phase lead (°)	Harmonic constituents	Harmonic constants H (mb)*	G (°)	K (°)
0.8932	1.2776	-0.0802	1.2801	-3.6	Q_1	5.2	242.6	96.9
0.9295	1.2686	-0.2143	1.2866	-9.6	O_1	30.7	251.7	106.0
0.9661	1.2326	-0.3405	1.2788	-15.4	M_1	2.3	256.2	110.5
0.9973	1.1862	-0.4211	1.2587	-19.5	P_1	15.5	264.6	118.9
1.0027	1.1771	-0.4316	1.2537	-20.1	K_1	48.4	266.4	120.7
1.0393	1.1136	-0.4686	1.2082	-22.8	J_1	3.1	278.9	133.2
	Predicted variance 1923 mb^2		SE = 0.8%	0.4°				
1.8591	1.0653	-0.3383	1.1177	-17.6	μ_2	2.5	239.1	307.7
1.8960	1.0198	-0.3607	1.0817	-19.5	N_2	21.6	259.9	328.5
1.9323	1.0036	-0.4588	1.1035	-24.6	M_2	108.8	284.3	352.9
1.9689	1.0194	-0.6138	1.1900	-31.1	L_2	2.7	310.5	19.1
2.0000	1.0559	-0.7661	1.3045	-36.0	S_2	36.5	316.0	24.6
2.0055	1.0641	-0.7930	1.3271	-36.7	K_2	9.4	313.2	21.8
	Predicted variance 6330 mb^2		SE = 0.7%	0.4°				

*1.00 mb ≈ 1.01 cm sea water

Total recorded variance	8265.4 mb^2
Total predicted variance	8253.9 mb^2 = 99.86%
Residual variance	11.5 mb^2

Table 5.--Response analysis for current station 2, north component, centimeters per second.
(Reference series in millibars)

Reference: "Predicted" tide station 1

July 25, 1972 to August 23, 1972
(29 days)

$X_2^{1,2}(0)$ (Species 1 & 2)
"Predicted" bilinear current
$Y_2^{1,2}(0)$ $Y_2^{2}(0)$ (Species 3 & 4)

Lat. 59°22.2N
Long. 146°13.8W
Depth 110 meters

Frequency (CPD)	Admittance, station to reference REAL	IMAG	Amplitude (R)	Phase lead (°)	Harmonic constituents	Harmonic constants H (cm/s)	G (°)	K (°)
0.9295	-0.0052	0.0372	0.0375	97.9	O_1	1.2	153.8	7.6
1.0027	-0.0052	0.0372	0.0375	97.9	K_1	1.8	168.5	22.3
	Standard error +41%			±23°				
	Recorded variance 4.12							
	Predicted variance 2.66							
	Residual variance 1.48							
1.8960	0.0701	0.0134	0.0713	10.8	N_2	1.5	249.1	316.6
1.9323	0.0701	0.0134	0.0713	10.8	M_2	7.8	273.5	341.0
2.0000	0.0701	0.0134	0.0713	10.8	S_2	2.6	305.2	12.7
	Standard error +24%			±14°				
	Recorded variance 38.30							
	Predicted variance 33.58							
	Residual variance 4.76							
3.8645	-0.0026	0.0271	0.0273	95.4	M_4	1.6	91.6	226.6
3.9323	-0.0026	0.0271	0.0273	95.4	MS_4	0.6	123.3	258.3
	Standard error +43%			±24°				
	Recorded variance 3.38							
	Predicted variance 2.08							
	Residual variance 1.30							

Total recorded variance 60.41
Total predicted variance 38.32 = 63.5%
Total residual variance 22.09

Table 6.--Response analysis for current station 2, east component, centimeters per second.
(Reference series in millibars)

Frequency (CPD)	Admittance, station to reference: REAL	IMAG	Amplitude (R)	Phase lead (°)	Harmonic constituents	Harmonic constants: H (cm/s)	G (°)	K (°)
0.9295	0.0767	0.0556	0.0947	36.0	O_1	2.9	215.7	69.5
1.0027	0.0767	0.0556	0.0947	36.0	K_1	4.6	230.4	84.2
	Standard error +29%			±17°				
	Recorded variance 20.96							
	Predicted variance 16.85							
	Residual variance 3.85							
1.8960	0.0648	-0.0705	0.0957	-47.4	N_2	2.1	307.3	14.8
1.9323	0.0648	-0.0705	0.0957	-47.4	M_2	10.4	331.7	39.2
2.0000	0.0648	-0.0705	0.0957	-47.4	S_2	3.5	3.4	70.9
	Standard error +30%			±17°				
	Recorded variance 74.69							
	Predicted variance 60.42							
	Residual variance 14.27							
2.9350	-0.0311	0.0070	0.0319	167.4	MK_3	1.5	34.7	316.0
	Standard error +47%			±27°				
	Recorded variance 3.58							
	Predicted variance 1.88							
	Residual variance 1.70							
3.8645	-0.0299	0.0278	0.0408	137.1	M_4	4.4	166.3	301.3
3.9323	-0.0299	0.0278	0.0408	137.1	MS_4	1.5	198.0	333.0
	Standard error +18%			±10°				
	Recorded variance 16.27							
	Predicted variance 15.12							
	Residual variance 1.15							

Total recorded variance 149.08
Total predicted variance 94.27 = 63.2%
Total residual variance 54.81

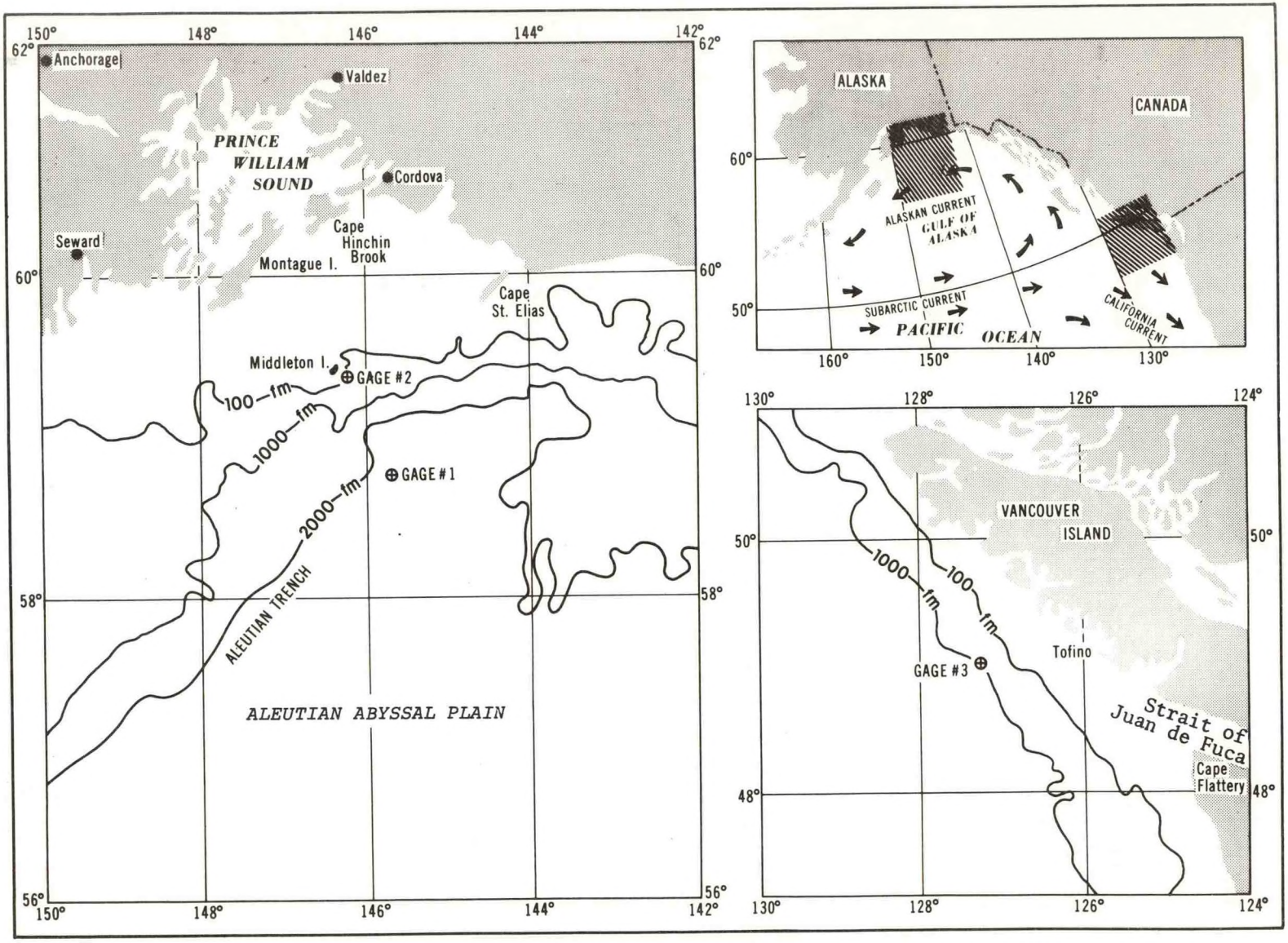

Figure 1.--Deployment sites of the deep sea tide and current measuring system.

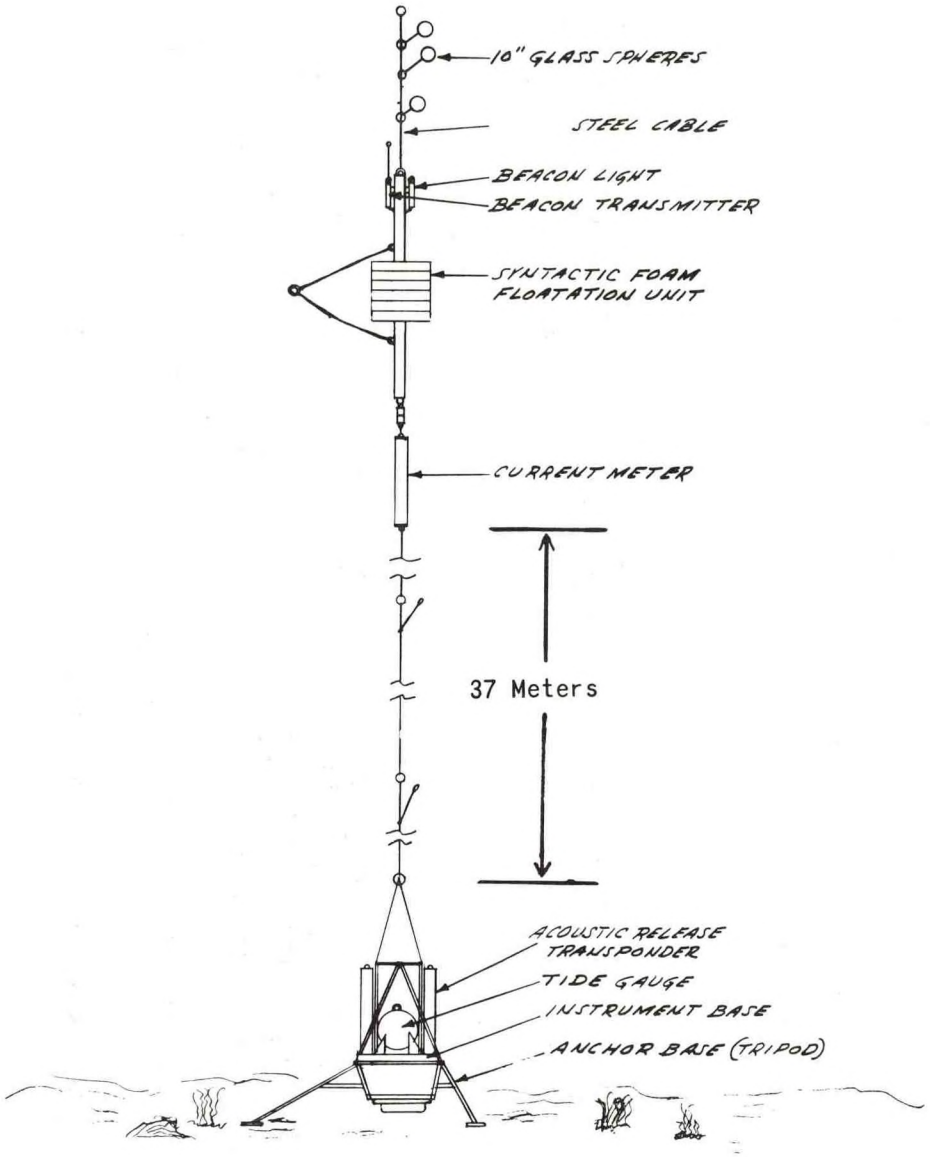

Figure 2.--Mooring configuration of the deep sea tide and current measuring system.

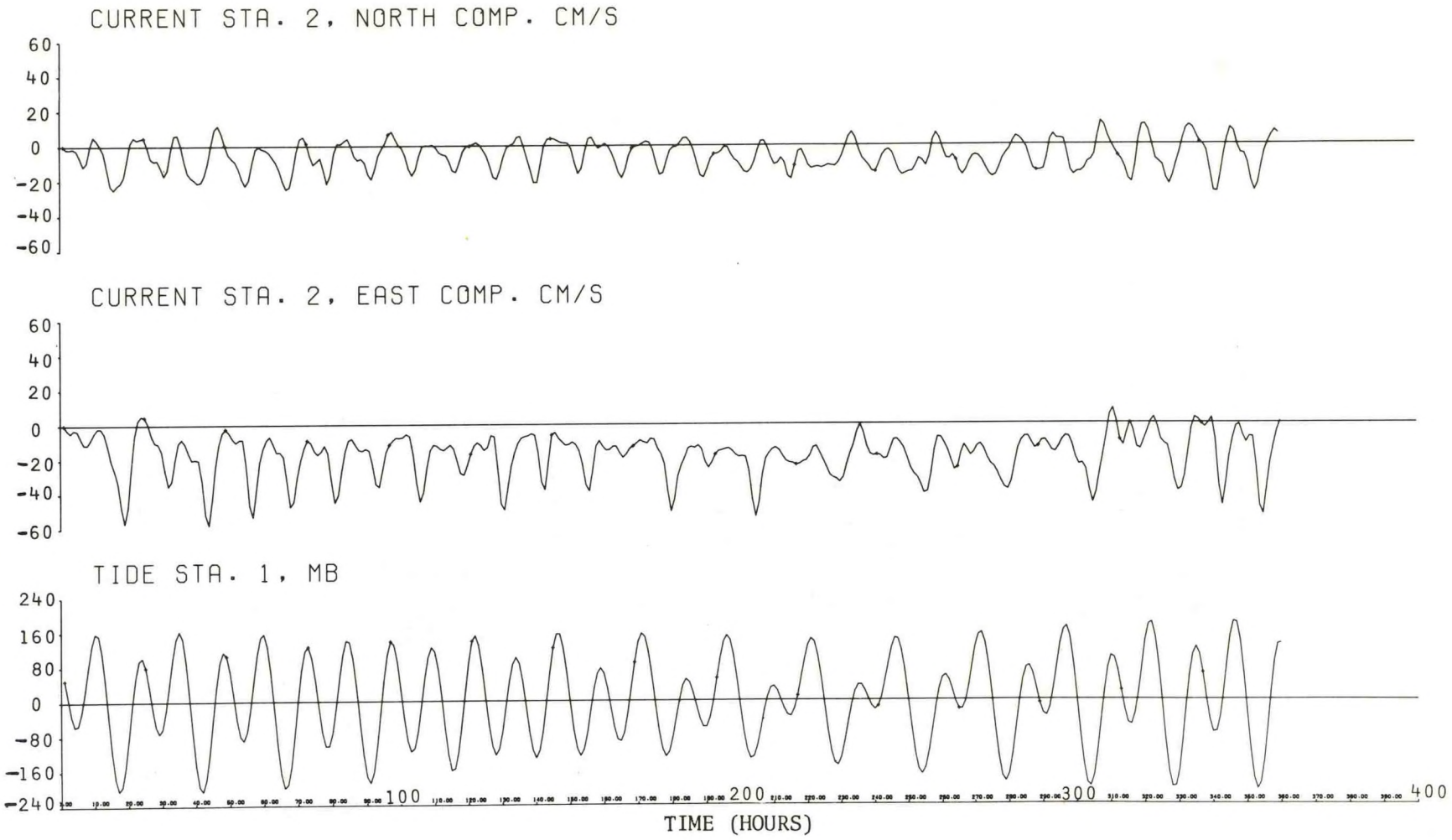

Figure 3.--Plots of 15-day samples of tide and current data, Gulf of Alaska stations.

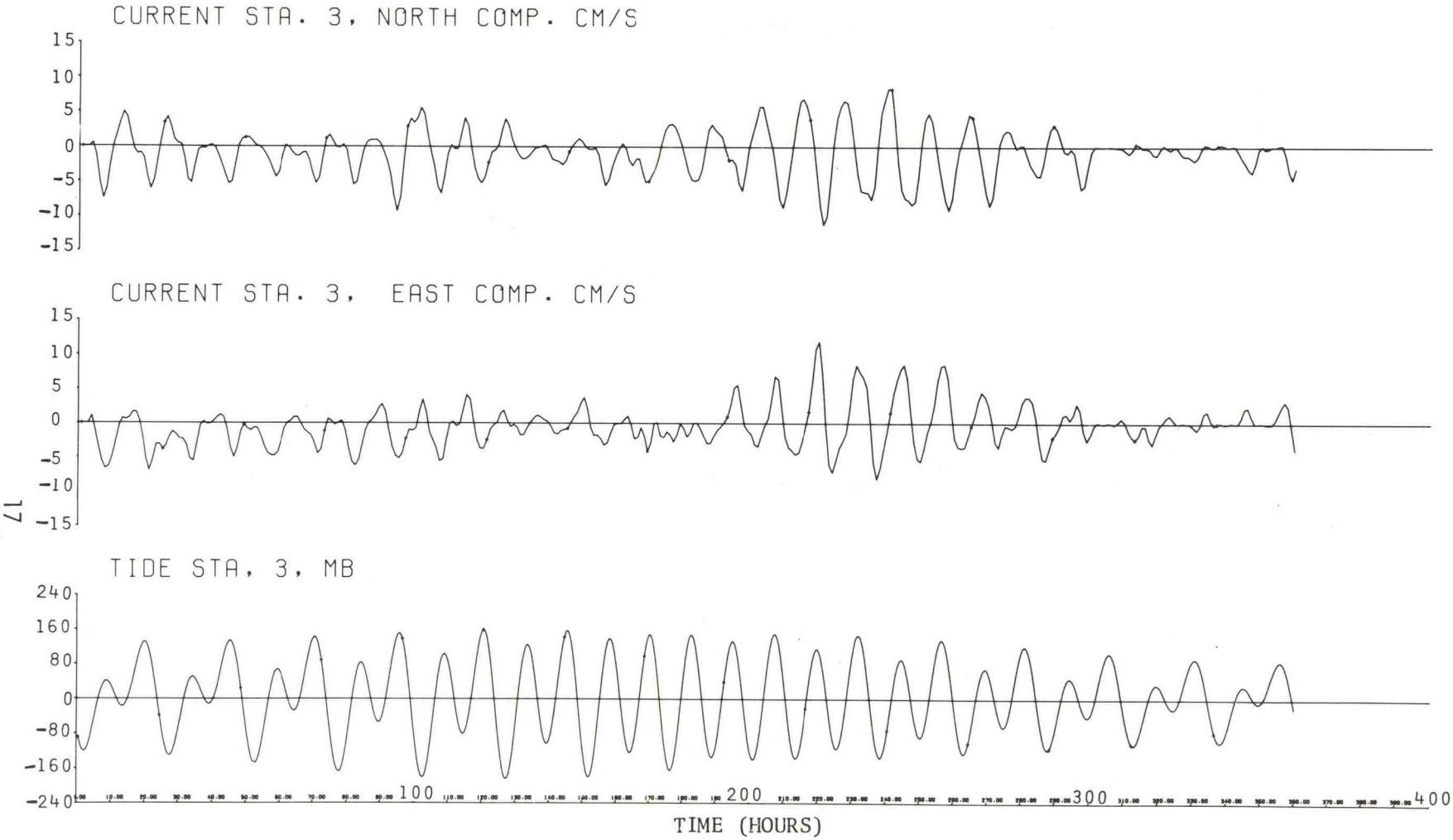

Figure 4.--Plots of 15-day samples of tide and current data, Gulf of Alaska stations.

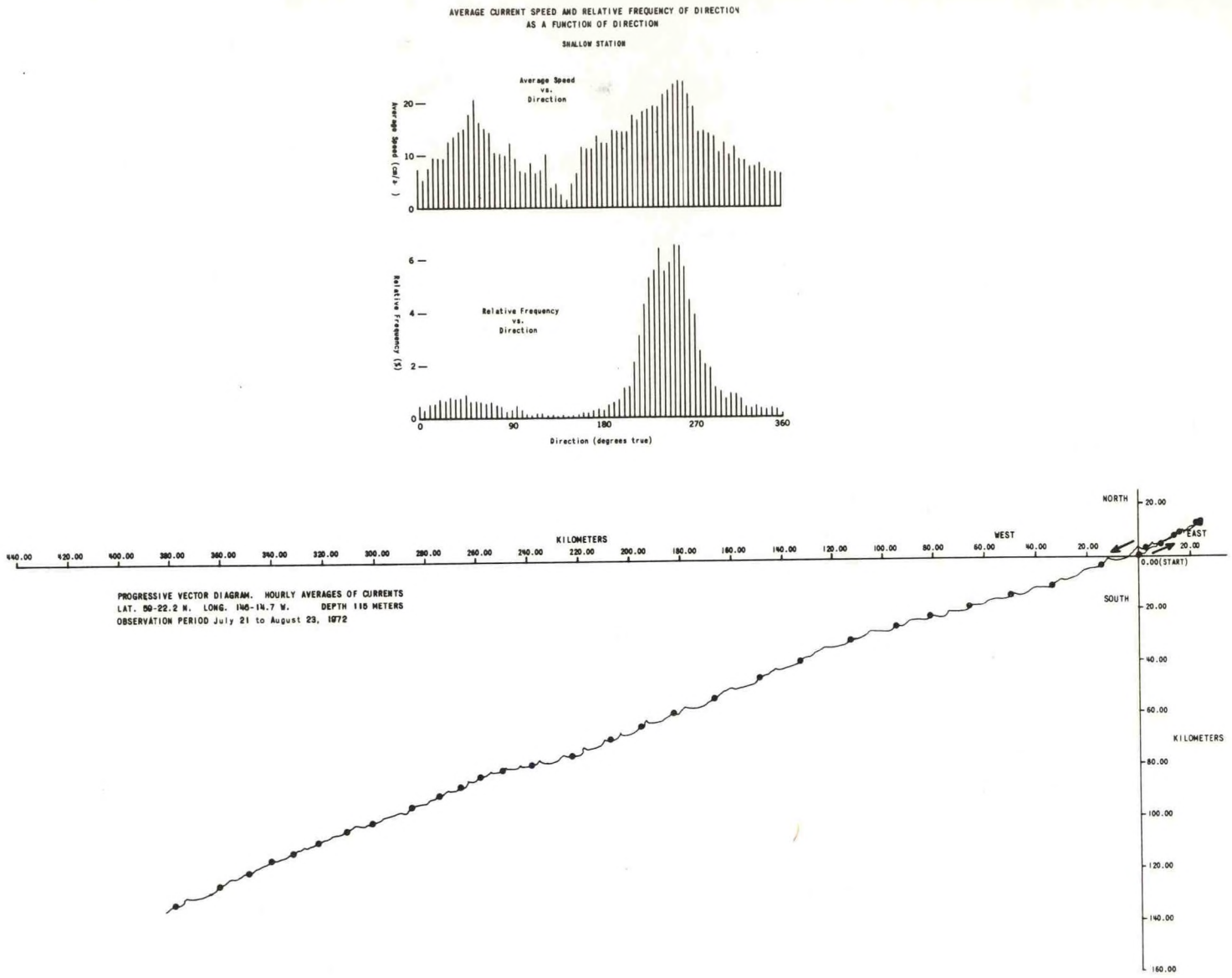

Figure 5.--Progressive vector diagram, current station 2 (Gulf of Alaska).

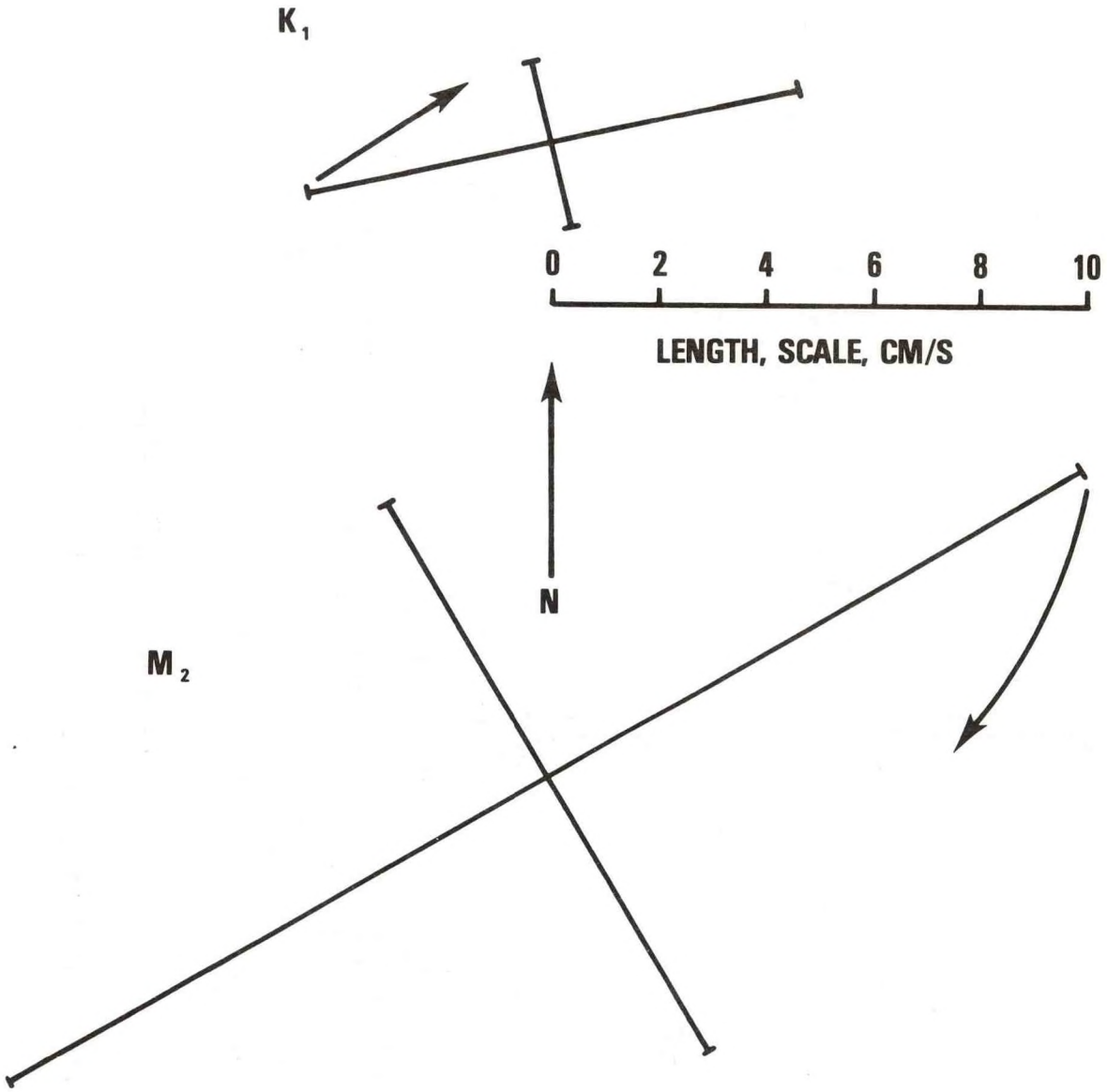

Figure 6.--Tidal current ellipses, current station 2 (Gulf of Alaska).

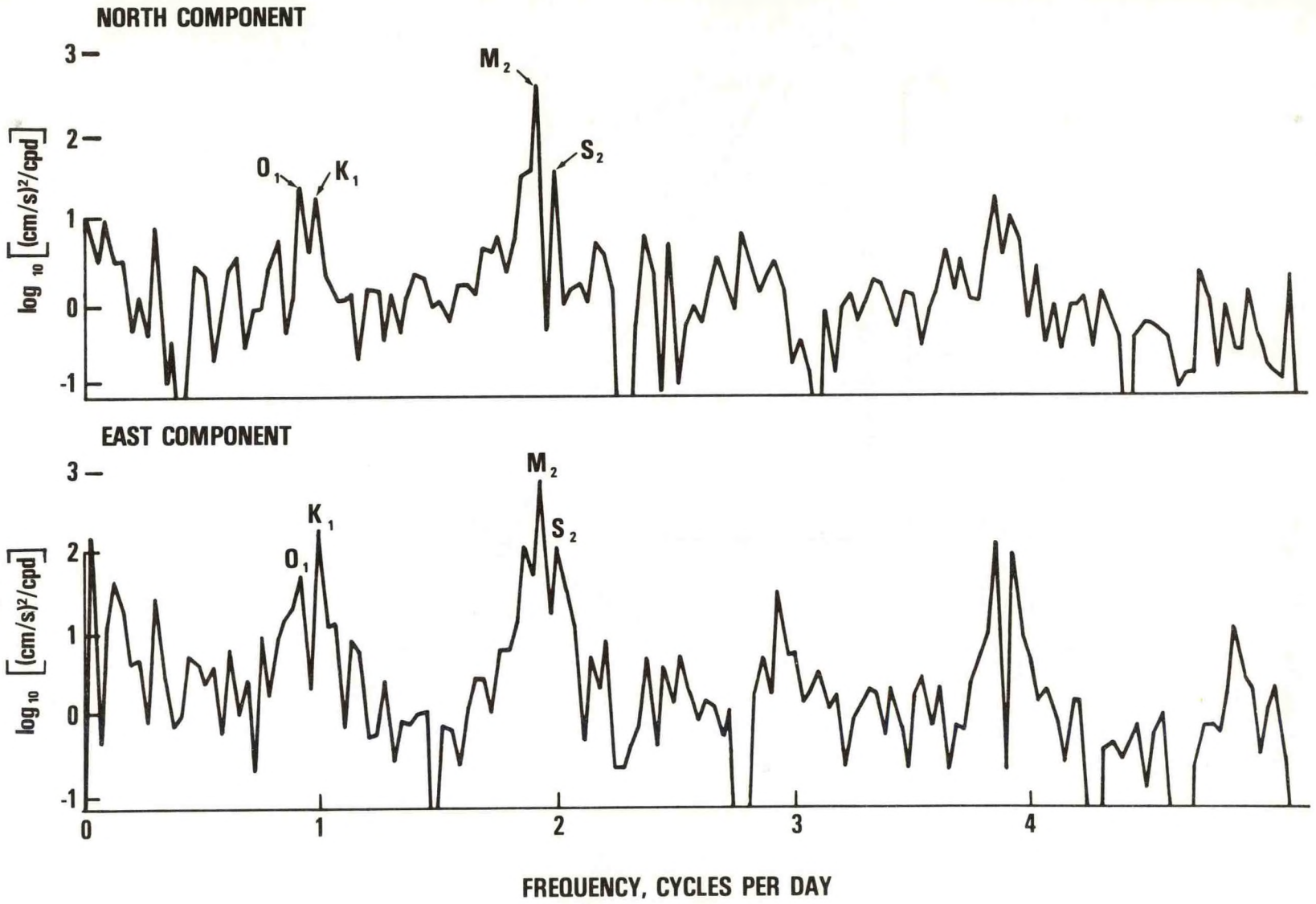

Figure 7.--Energy spectra (periodograms), north and east components current station 2.

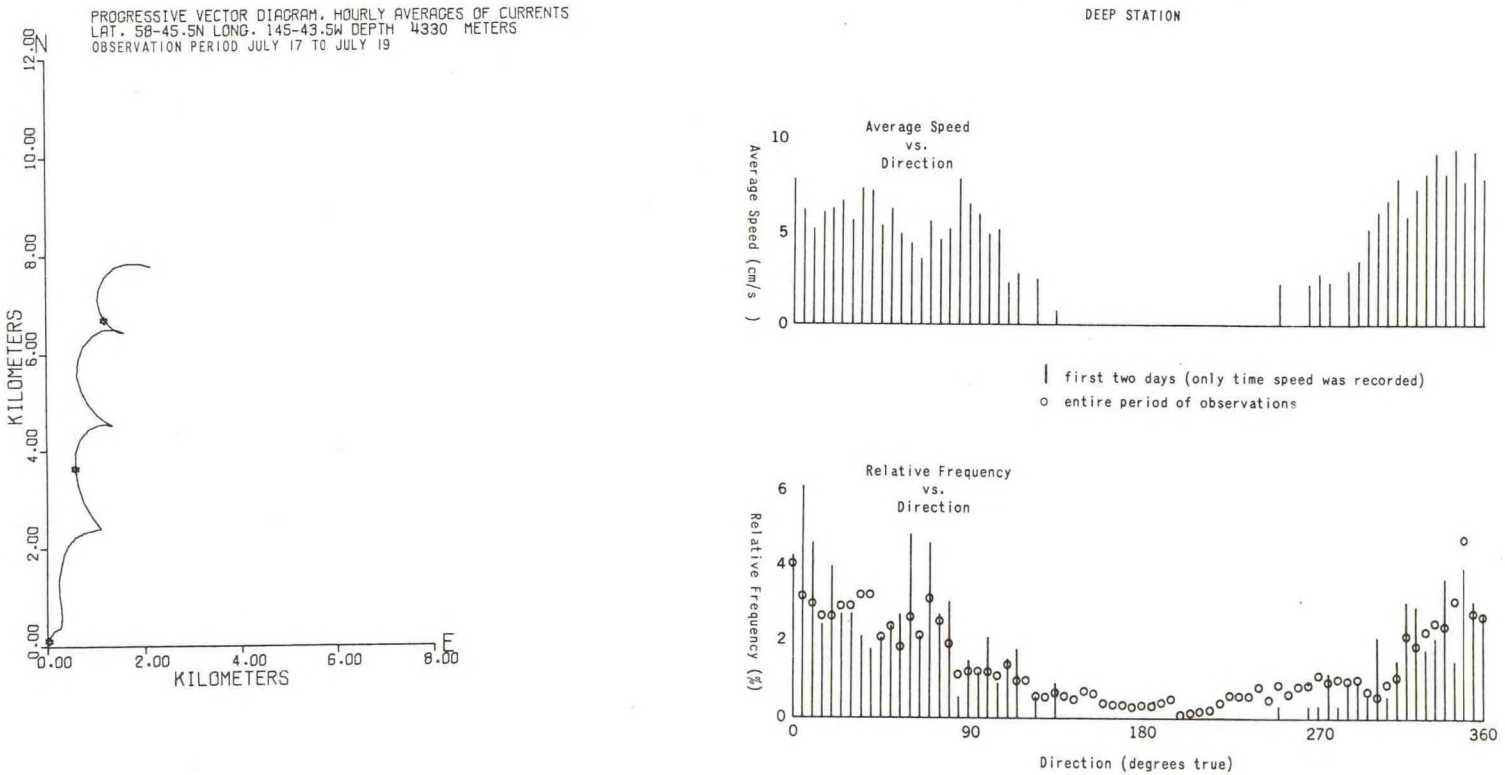

Figure 8.--Progressive vector diagram and relative frequency diagrams, current station 1 (Gulf of Alaska).

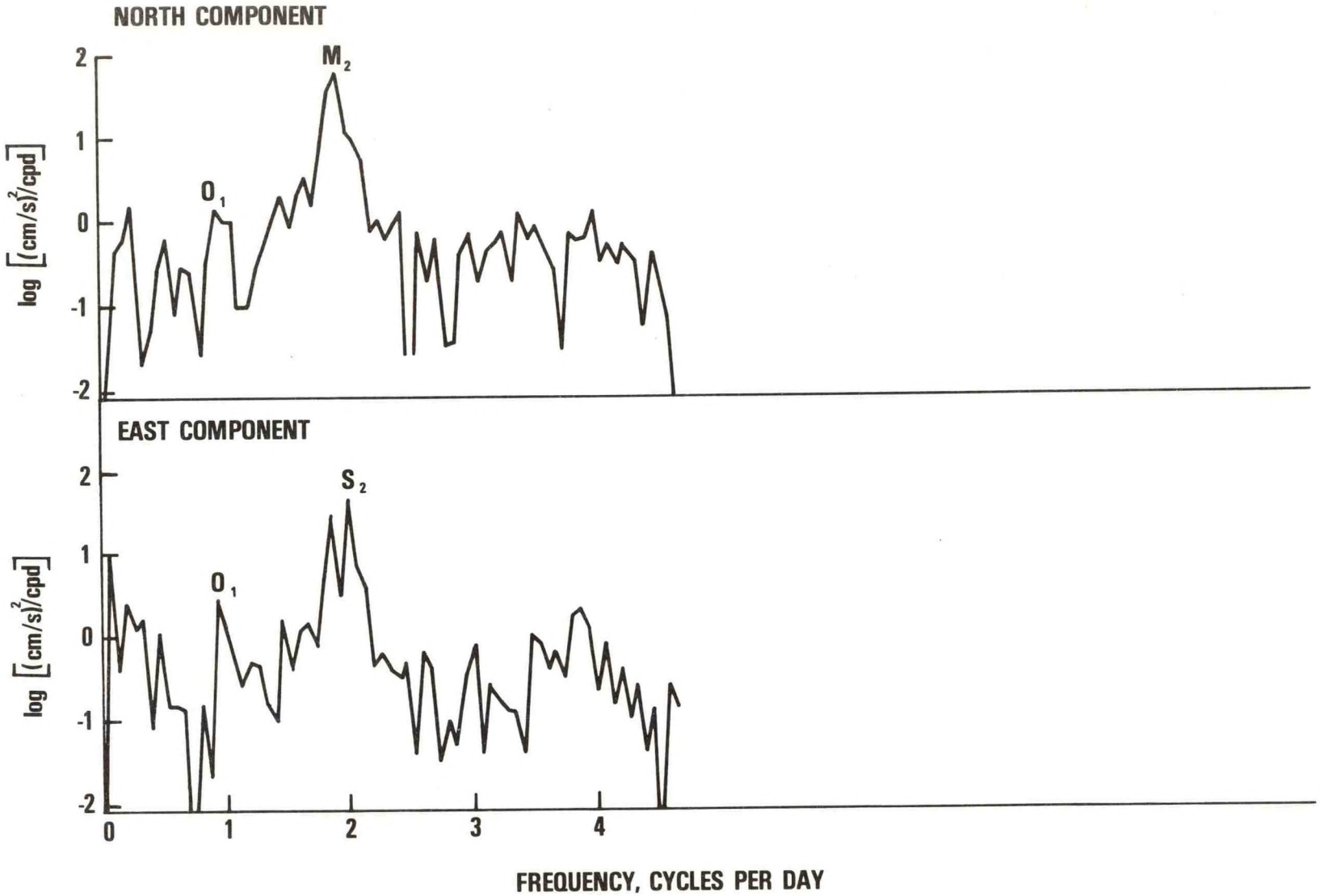

Figure 9.--Energy spectra (periodograms), north and east components current station 3, (offshore Vancouver Is.).

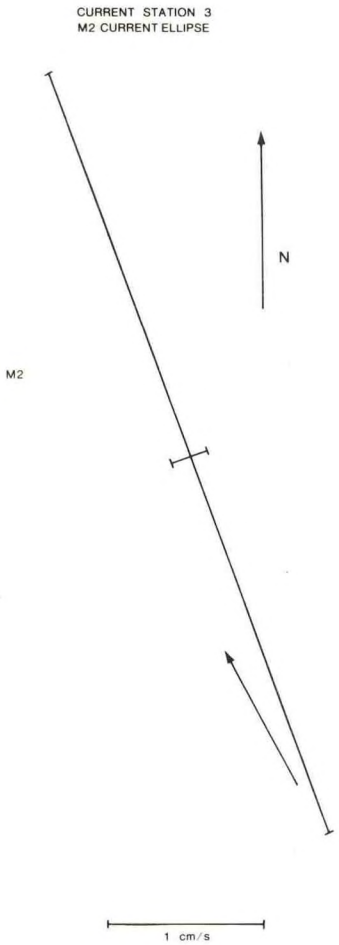

Figure 10.--M_2 tidal current ellipse, current station 3 (offshore Vancouver Is.).

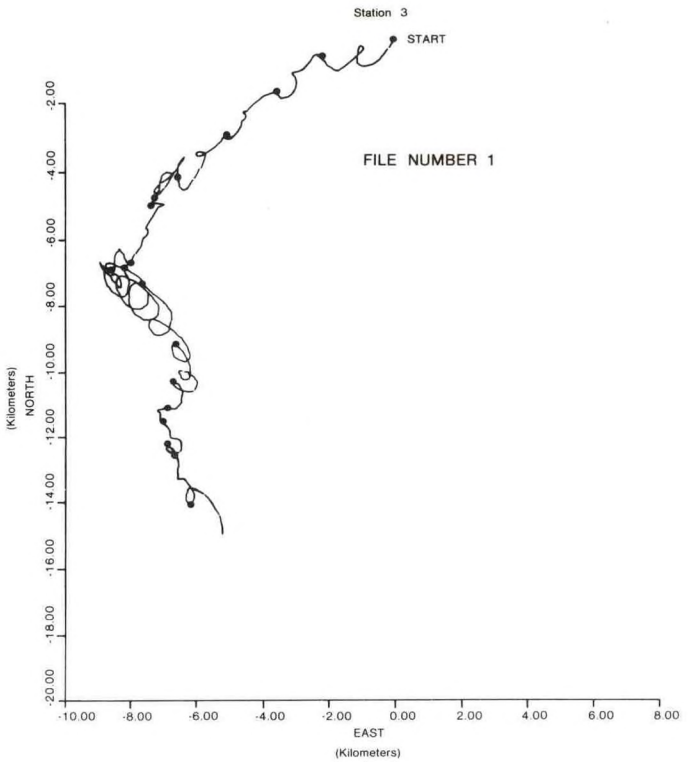

Figure 11.--Progressive vector diagram, current station 3 (offshore Vancouver Is.).